ARTICLE

Real-Time Observation of Pyoverdine Dissolving Ferric Hydroxide

Jia-hong Li*

Hefei National Laboratory for Physical Sciences at the Microscale, University of Science and Technology of China, Hefei 230026, China

(Dated: Received on May 25, 2016; Accepted on June 9, 2016)

Pyoverdine is one of the siderphores excreted by *Pseudomonas aeruginosa* that can help microbe to uptake iron *in vitro*. To determine the effect of pyoverdine chelating with iron, we purified the free pyoverdine and applied the dynamic laser light scattering (DLS) to detect the interaction between the pyoverdine and ferric hydroxide. The real-time DLS data analysis indicated that pyoverdine can directly combine with $Fe(OH)_3$ to form complexes and these substances are gradually degraded by themselves then completely disappeared. In our experiment, we have demonstrated that pyoverdine may not only chelate ferric ion but also availably dissolve ferric hydroxide which assists bacteria to survive in iron-deficient environments.

Key words: Pyoverdine, Ferric hydroxide, Dissolution, Dynamic laser light scattering

I. INTRODUCTION

Iron plays an essential role in the growth and reproduction of most microorganisms, since a substantial fraction of enzymes requires the metal ion as their catalysis centers. To be more specifically, a systematic analysis of 310 redox-dependent enzymes data shows that 30% of enzymes contain metal iron as redox centers. And iron acts as a cofactor involved in most cellular processes such as electron transfer, RNA synthesis and resistance to reactive oxygen intermediates [1, 2]. Although iron is the fourth most abundant element on the earth's surface, its bioavailability is limited in aqueous environments [3]. The majority of Fe^{3+} forms ferric oxide hydrate complexes ($Fe_2O_3{\cdot}nH_2O$) in the existance of oxygen and water at the physiological pH. The concentration of free ferric ions is from 10^{-9} mol/L to 10^{-18} mol/L since these complexes are quite stable [4]. In order to acquire the ferric ions in environments, bacteria, fungi and plants secrete the low-molecular-weight secondary metabolites termed siderphores (200−2000 Da) as iron chelating agents to facilitate absorption of the iron *in vitro* [5–7].

Pseudomonas aeruginosa is responsible for chronic infections in the pathogenesis of cystic fibrosis (CF) [8]. Under iron-deficient environments, *Pseudomonas aeruginosa* can produce the yellow-green, fluorescent, water-soluble pigments termed pyoverdine (Fig.1) to acquire ferric ions. Pyoverdines have extremely high affinity for Fe^{3+} ion with stability constant in general around 10^{32} mol/L [9]. Although pyoverdines were discovered more than 120 years ago [10], the function of iron acquisition was identified by Meyer and Abdallah until 1978 [11]. And in the late 1980s and early 1990s, the structure of pyoverdines were analyzed using the NMR and mass spectrometry techniques [12–15]. Pyoverdine not only plays the role as iron-scavenger in *Pseudomonas aeruginosa*, but also regulates the production of at least three virulence factors including exotoxin A, an endoprotease, and pyoverdine itself, all of them are major contributors for the bacterial infections [16]. Furthermore, to some extent, pyoverdine can also protect the bacteria from metal toxicity and the ROS which lead to deadly harm to microbe [4, 7, 17]. As for application, pyoverdine can serve as biological recognition elements for the fluorescent detection such as ferric ion, furazolidone and copper ion in environment [18–20].

In previous research, the classical or stopped-flow spectrophotometry analysis suggested that the reaction of the free pyoverdine chelates with the monohydroxylated Fe^{3+} species $Fe(OH)^{2+}$ to form the ferric-pyoverdine complexes, and these data was supported by the dissociative Eigen-Wikin mechanism [9, 21]. However the *in situ* infrared spectroscopy confirmed that pyoverdine catechol ligand can directly interact with the TiO_2 and Fe_2O_3 surfaces by the covalent bonding aqueous environment [22, 23]. So it remains unknown for the mechanism of the pyoverdine acquiring the insoluble iron.

In this work, we used the laser light scattering (LLS) to detect the interactions between the pyoverdine and insoluble ferric hydroxide colloids. Our experiments also reveal that iron plays a highly significant role in *Pseudomonas aeruginosa* growth and pyoverdine production.

*Author to whom correspondence should be addressed. E-mail: lijh2013@mail.ustc.edu.cn

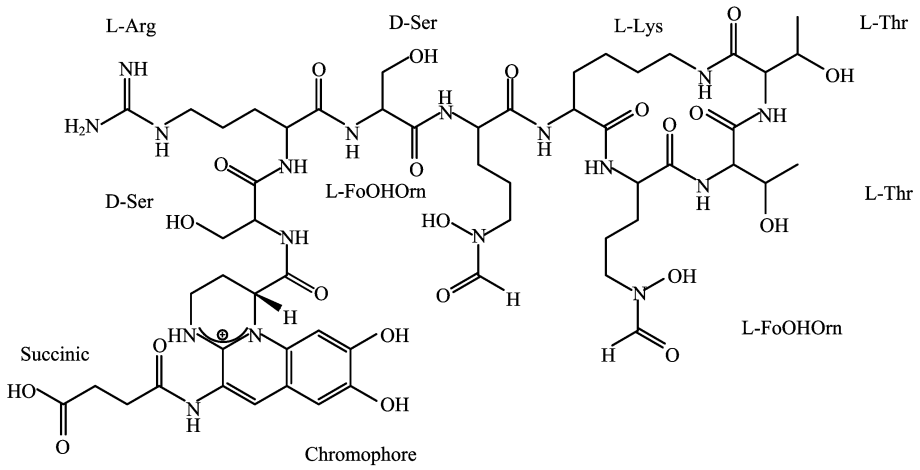

FIG. 1 The structure of pyoverdine produced by *Pseudomonas aeruginosa* ATCC 15692 with three chelation sites, which includes two hydroxamic acids and a dihydroxyquinoline-type function.

II. EXPERIMENTAL PROCEDURES

A. Microorganisms and pyoverdine production

The strains used in this experiment were the *Pseudomonas aeruginosa* ATCC 15692 and the *Pseudomonas aeruginosa* PAO1. The iron-limited culture medium termed synthetic succinate medium (SSM) had following composition: 7.86 g/L $K_2HPO_4{\cdot}3H_2O$, 3 g/L KH_2PO_4, 1 g/L $(NH_4)_2SO_4$, 0.2 g/L $MgSO_4{\cdot}7H_2O$, 4 g/L succinic acid. The medium was adjusted to pH=7.0 by 1 mol/L NaOH before sterilization [9]. The 1 L culture medium was dispensed into 1 L conical flasks, each of them contained 200 mL of medium. The flasks were inoculated 10 mL of *Pseudomonas aeruginosa* ATCC 15692 which grew to exponential-phase in aerobic condition at 37 °C and 220 r/min in a shaker-incubator. After 17 h, the culture medium was centrifuged at 10000×g for 10 min at 4 °C. In order to get the bacteria-free crude pyoverdine solution, the supernatant was filtered by 0.22 μm membranes (Merck Millipore) [24].

B. Pyoverdine isolation and purification

Pyoverdine isolation and purification were carried out as a published procedure with some modifications [24]. In brief, the cell-free supernatant was buffered with 1 mol/L HEPES (*N*-2-hrydroxyethylpiperazine-*N*′-ethanesulfonic acid) buffer to pH=7.0 and then applied to a chelating Sepharose fast flow column (1.6×2.5 cm, 5 mL; GE Healthcare). This column was pre-saturated with $CuSO_4$ and equilibrated with 20 mmol/L HEPES buffer (pH=7.0) containing 100 mmol/L NaCl. The eluent flow rate was set at 300 mL/h. The column was then washed with 50 mL of 20 mmol/L HEPES buffer and eluted with 20 mmol/L acetate buffer (pH=5.0) containing 100 mmol/L NaCl. Per 5 mL fraction was collected and the A_{400} absorbance spectroscopy was measured by NanoDrop 2000 Spectrophotometer (Thermo SCIENTIFIC) to determine pyoverdine-Cu containing. The pyoverdine-containing fractions were pooled separately and lyophilized.

Each of the fractions dried pyoverdine was dissolved in 1 mL 10 mmol/L EDTA and then applied to a Sephadex G-15 column (1 cm×80 cm, GE Healthcare) that had been pre-equilibrated with deionized water. The column was eluted with ultrapure water at a flow rate of 20 mL/h and 15 fractions (4 mL) were collected and the absorbance of UV-Vis spectrum (190−1000 nm) was monitored. The fractions with the highest absorbance at 385 nm were chosen as purified-pyoverdine and the samples were pooled, lyophilized, and stored at −20 °C.

C. Preparation of the samples for DLS characterization

The purified-pyoverdine was dissolved into 0.1 mol/L phosphate buffered saline (PBS) to final concentration to 25, 50, 100 μmol/L at physiological pH 7.4 and then the dust in solution was filtered by 0.45 μm membrane (Millipore). The absorption spectrum of the free pyoverdine was measured by UV-Vis spectrum at 25 °C. The concentration of the free-pigment was calculated using the extinction coefficients λ_{max}=385 nm and ε=16500 $(mol/L)^{-1}cm^{-1}$ [11]. And the Fe^{3+} source was obtained from the 1 mmol/L $FeCl_3$ solution pH 2.0 which was filtered by 0.45 μm membrane. In a typical experiment, a proper volume of the dust-free $FeCl_3$ was directly added into the dust-free free pyoverdine PBS buffer to start the biodegradation of ferric hydroxide.

D. Laser light scattering

A modified commercial LLS spectrometer (ALV/DLS/SLS-5022F) equipped with an ALV5000

DOI:10.1063/1674-0068/30/cjcp1605114

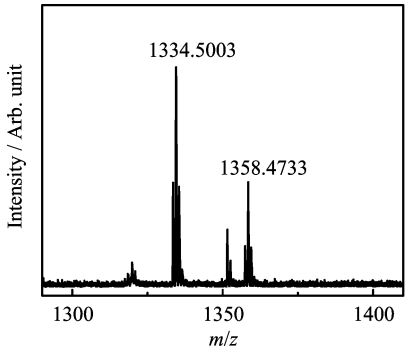

FIG. 2 MALDI-TOF MS spectrum of pyoverdine purified from *Pseudomonas aeruginosa* ATCC 15692.

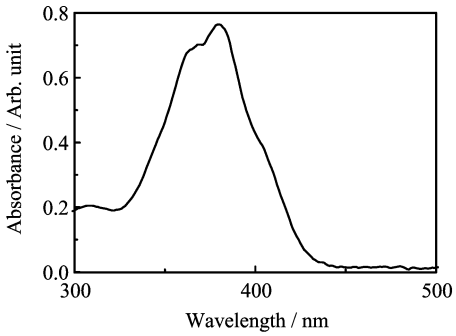

FIG. 3 UV-Vis spectrum of pyoverdine purified from *Pseudomonas aeruginosa* ATCC 15692 (the concentration of pyoverdine was 440 μmol/L).

multi-τ digital time correlator and a cylindrical solid-state He-Ne laser (UNIPHASE, out power=22 mW at λ_0=632.8 nm) as the light source was used. In dynamic LLS, the self-beating mode of the intensity-intensity time auto-correlation function $G^{(2)}(t, \mathrm{q})$ was measured where t is related to the delay time and q represents the scattering vector [25–27]. The line-width distribution $G(\Gamma)$ is accompanied with the analysis of $G^{(2)}(t, \mathrm{q})$. For a pure diffusive relaxation, Γ is connected with the translational diffusion coefficient distribution $G(D)$ or a hydro-dynamic radius distribution $f(R_\mathrm{h})$ via the Stock-Einstein equation: $R_\mathrm{h}=(k_\mathrm{B}T/6\pi\eta_0)/D$, where k_B, T and η_0 are the Boltzmann constant, the absolute temperature and the solvent viscosity, respectively [28]. According to the definition of Rayleigh scatter ratio $R_\mathrm{vv}(q)$ which is concerned with the scatter particles property, size and concentration. In the dilute solution, $R_\mathrm{vv}(q)$ can be related to the weight-average molar mass M_w, the second virial coefficient A_2, and the root-mean square z-average radius $\langle {R_\mathrm{g}}^2 \rangle_z^{1/2}$ by

$$\frac{KC}{R_\mathrm{vv}(q)} = \frac{1}{M_\mathrm{w}}\left(1+\frac{1}{3}q^2\left\langle R_\mathrm{g}^2\right\rangle_z q^2\right)+2A_2C \quad (1)$$

$$K = \frac{4\pi^2 n^2(\mathrm{d}n/\mathrm{d}C)^2}{N_\mathrm{A}{\lambda_0}^4} \quad (2)$$

$$q = \frac{4\pi n}{\lambda_0}\sin\frac{\theta}{2} \quad (3)$$

Where $\mathrm{d}n/\mathrm{d}C$, n, N_A, λ_0 represent the specific refractive index increment, Avogadros number, the solvent refractive index, and the vacuum light wavelength. Since when $C\to 0$ and $q\to 0$, $R_\mathrm{vv}\approx KCM_\mathrm{w}$ [28]. In this study, we used a fixed angle (30°) to obtain all data and the concentrations of Fe^{3+} and free-pyoverdine were both at micro molar level.

E. Bacteria growth rate and pyoverdine production measurement

The various contents of iron culture mediums were prepared by adding different volume of 1 mmol/L $FeCl_3$ (pH=2.0) into the solution containing 50 μmol/L free pyoverdine or not SSM. In order to assure that the initial quantity of bacteria was consistent, the strain of *Pseudomonas aeruginosa* PAO1 was cultured to exponential-phase in aerobic condition at 37 °C and 220 r/min. The 10 μL of the bacteria was inoculated into the 1 mL fresh SSM and the growth rate of bacteria was monitored every 2 h by measuring the optical density at 600 nm (OD_{600}) by eppendorf biophotometer plus (Thermo Fisher SCIENTIFIC).

III. RESULTS AND DISCUSSION

A. Characterization of the free-pyoverdine

The purified pyoverdine can be characterized with the mtrix-assisted laser desorption ionization time of flight mass spectrometry (MALDI-TOF MS) (Fig.2) to obtain the intact siderphore molar mass and the UV-Vis spectrum (Fig.3) to identify free-pyoverdine. The MALDI-TOF MS gave compound molecular ion M^+ at m/z=1334.5003 which was coincided with the simulation of the free pyoverdine via Chemoffice 2015 and the previous reports [13]. And the absorption spectrum of free pyoverdine in water solution could be observed at 385 nm while the Fe-pyoverdine complexes had the largest peak at 403 nm according to the reported data in Ref.[11], so we acquire the metal free pyoverdine.

B. The stability of iron hydroxide colloids

Considerable evidence suggests that iron participates in many bacterial processes while the amount of free iron in aerobic aqueous environments (pH=7.0) is less than 10^{-17} mol/L [29]. To understand the ferric hydroxide colloids stability, dynamic laser lighting scatter (DLS) was applied to observe the different contents of iron in the 0.1 mol/L PBS buffer (pH=7.40) at room temperature. Subsequently, the sizes of insoluble $Fe(OH)_3$ colloids were measured for more than 12 h (Fig.4 (a) and (b)). The average hydrodynamic radius $\langle R_\mathrm{h}\rangle$ of the insoluble ferric hydroxide colloids in 0.1

DOI:10.1063/1674-0068/30/cjcp1605114

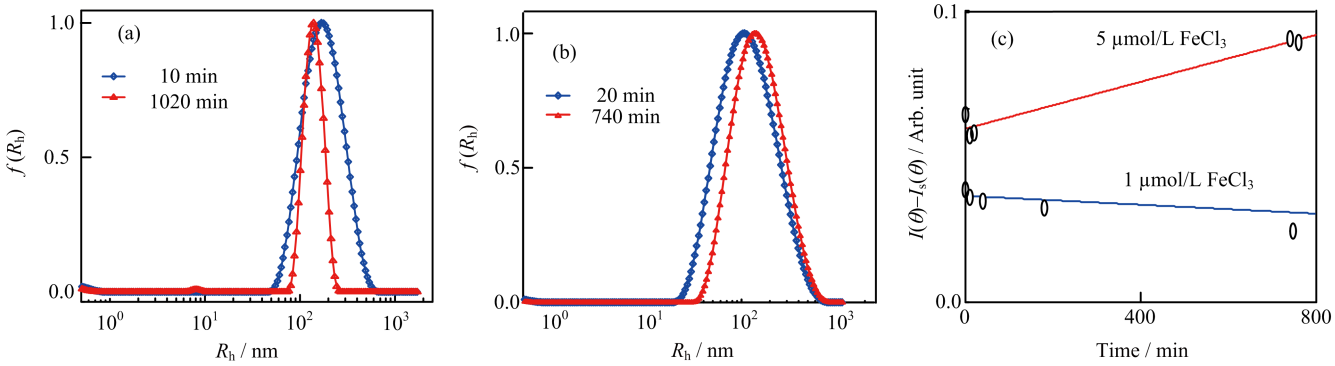

FIG. 4 The $\langle R_h \rangle$ distribution of the $Fe(OH)_3$ colloids at the different time, where the iron contents are (a) 1 μmol/L and (b) 5 μmol/L in 0.1 mol/L PBS buffer (pH=7.40, 25 °C). (c) The time dependence of the $Fe(OH)_3$ colloids scattering intensity ($\langle I(\theta)-I_s(\theta) \rangle$) in PBS buffer, where the Fe^{3+} contents are 1 and 5 μmol/L, respectively.

TABLE I Characterization of different Fe^{3+} contents in PBS samples. $C_{Fe^{3+}}$: Fe^{3+} content, $t_{obs.}$: observation time.

$C_{Fe^{3+}}$/(μmol/L)	$t_{obs.}$/min	$\langle R_h \rangle$/nm	PDI
1	10	190	0.164
1	1020	194	0.387
5	10	104	0.289
5	740	134	0.230

mol/L PBS buffer changed a little during the observation. The results are summarized in Table I. Figure 4(c) shows the ferric hydroxide colloids contents in the samples which scattering intensity variation is expressed as $\langle I(\theta)-I_s(\theta) \rangle$, where $I(\theta)$ and $I_s(\theta)$ are respectively defined as the solution intensity and the pure solvent intensity which were recorded under the same conditions. As Fig.4(c) shows the intensity of the $Fe(OH)_3$ colloids changed slightly during the observation time. These results suggest that most of iron exists in the form of ferric hydroxide colloids in the aqueous environment and the state of insoluble iron colloids is quite stable because the ferric ions have higher precipitation dissolution equilibrium constant.

C. *Pseudomonas aeruginosas* use the insoluble iron in environment

Since the ferric hydroxide colliods are very stable in environment, the free Fe^{3+} is extremely restricted for bacterial uptake. To understand the relationship between the iron and the *Pseudomonas aeruginosa* growth better, we measured the bacterial population OD_{600} every 2 h in different Fe^{3+} contents SSM which were supplemented or not with 50 μmol/L free pyoverdine. Figure 5(a) shows that iron-rich environments help the bacteria to multiply vice versa. The amount of bacteria in iron-rich mediums (final contents of 5 μmol/L $FeCl_3$) were more than 22 times compared to iron-limited mediums (final contents of 0 μmol/L $FeCl_3$) after 10 h incubation. Interestingly, exogenous free pyoverdine in different iron contents SSM could promote bacteria reproduction and narrowed the gap in growth rate of the various iron contents (Fig.5(b)). The results suggest that the *Pseudomonas aeruginosa* proliferation rate increased with the iron contents increasing even in the ferric ions scarce conditions and free pyoverdine can facilitate bacterial reproduction. This observation indicates that bacteria can make full use of insoluble iron and bacteria may secrete some substances to dissolve ferric hydroxides for iron acquisition.

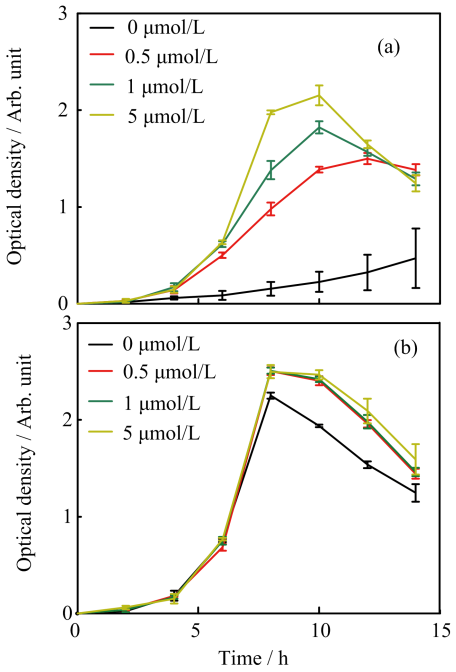

FIG. 5 Planktonic *Pseudomonas aeruginosa* PAO1 growth rate in different Fe^{3+} contents (0, 0.5, 1, 5 μmol/L) of SSM (a) without or (b) with 50 μmol/L free pyoverdine at 37 °C. Values are the mean of three independent assays. The error bars indicate the standard error of the mean.

DOI:10.1063/1674-0068/30/cjcp1605114

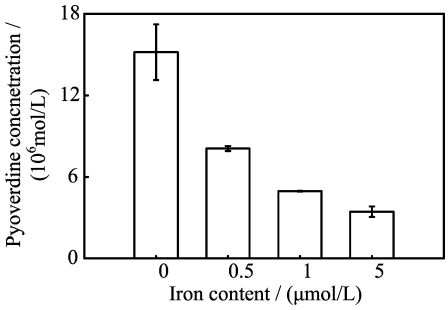

FIG. 6 The pyoverdine production in different Fe^{3+} contents (0, 0.5, 1, 5 μmol/L) of SSM after 14 h incubation. Values are the mean of three independent assays. The error bars indicate the standard error of the mean.

TABLE II Characterization data of different Fe^{3+} contents in 100 μmol/L pyoverdine samples. PDI: polymer dispersity index.

$C_{Fe^{3+}}$/(μmol/L)	$t_{obs.}$/min	$\langle R_h \rangle$/nm	PDI
1	10	408	0.251
	730	0	
5	20	290	0.184
	660	0	

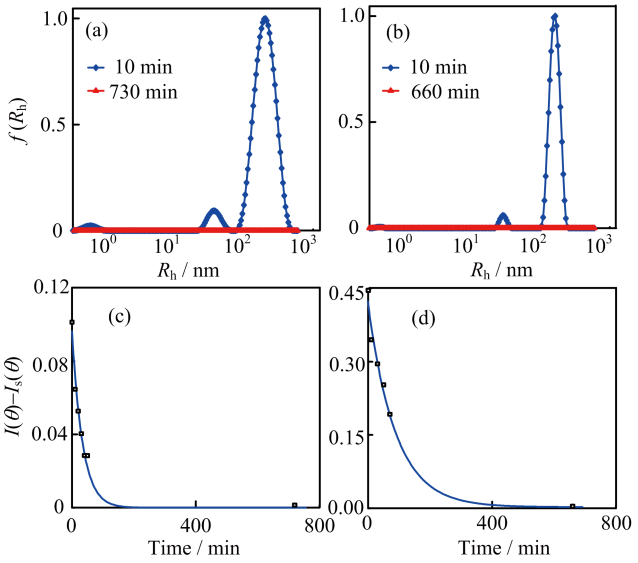

FIG. 7 The $\langle R_h \rangle$ distribution of the complexes at the different time after addition of $FeCl_3$ into 100 μmol/L pyoverdine PBS buffer, where the final iron content is (a) 1 μmol/L and (b) 5 μmol/L. The time dependence of the complexes intensity $\langle I(\theta)-I_s(\theta) \rangle$ in (c) 1 μmol/L and (d) 5 μmol/L Fe^{3+} contents PBS solution which contains 100 μmol/L pyoverdine.

D. Pyoverdine dissolves insoluble iron

To test this hypothesis, we first addressed the question, do bacteria always secreted the pyoverdine no matter the amount of iron contained in the culture mediums. The pyoverdine UV-Vis absorbtion was measured in bacterial centrifugal supernatant fluid after 14 h incubation. Figure 6 shows that the pyoverdine concentration without addition $FeCl_3$ medium was five times higher than addition $FeCl_3$ to final iron content of 5 μmol/L in SSM. These results indicate that bacterial pyoverdine secretion was reduced with the increasing iron contents in SSM. The data also suggest that even in iron-rich medium, bacteria still needs to synthesis pyoverdine in order to dissolve the ferric hydroxide colloids.

The chelation of pyoverdine and the ferric ion was identified by various groups [30]. Whether the interaction between the pyoverdine with insoluble ferric hydroxide remain mysterious. In order to observe the interaction between the pyoverdine and ferric hydroxide colloids, we used the dynamic laser light scattering to obtain the real-time data of the complexes $\langle R_h \rangle$ change as well as the solution intensity variation. As Fig.7 (a) and (b) shown that the $\langle R_h \rangle$ of initial insoluble complexes in containing pyoverdine PBS buffer were more than twice sizes larger than the same content iron added into the PBS buffer (Fig.4 (a) and (b)). The results were summarized in Table II. Figure 7 (c) and (d) show the scattering intensity $\langle I(\theta)-I_s(\theta) \rangle$ of the complexesin containing 100 μmol/L pyoverdine PBS buffer which final iron contents are 1 and 5 μmol/L, respectively. Most interestingly, the insoluble complexes disappeared after 200 and 400 min later since 1 and 5 μmol/L $FeCl_3$ addition into the containing pyoverdine PBS samples. And the intensity of the complexes which had exponential descent with the increased time for interaction between the pyoverdine and ferric hydroxide colloids. Furthermore, we also investigated the $\langle R_h \rangle$ distribution and the intensity of the iron complexes in different pyoverdine (25 and 50 μmol/L) concentrations samples where the final iron contents are 5 μmol/L (see Fig.8). The results were summarized in Table III. Figure 8 illustrates that the ferric hydroxide colloids still can be dissolved under the low concentration of pyoverdine conditions. And these results mean that the ferric hydroxide-pyoverdine complexes degrade themselves as soon as they formation. In contrast, the scattering intensity changed slightly in the same iron contents PBS buffer without pyoverdine (Fig.4(c)). Thus the free pyoverdine can interact with the ferric hydroxide colloids to form ferric hydroxide-pyoverdine complexes and the new complexes were unstable and gradually decomposed themselves. So pyoverdine can promote bacteria uptaking insoluble iron source in iron-deficient environments.

IV. CONCLUSION

In this work, we reveal that pyoverdine can directly interact with the $Fe(OH)_3$ colloids to form new complexes and gradually degraded themselves. Iron con-

DOI:10.1063/1674-0068/30/cjcp1605114

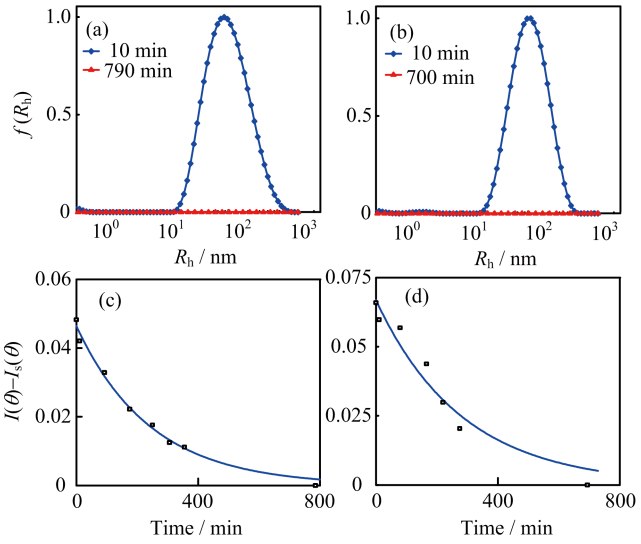

FIG. 8 The $\langle R_h \rangle$ distribution of the complexes at the different time after addition of 5 μmol/L $FeCl_3$ into (a) 25 μmol/L and (b) 50 μmol/L of pyoverdine PBS buffer. The time dependence of the complexes intensity $\langle I(\theta)-I_s(\theta) \rangle$ in (c) 25 μmol/L and (d) 50 μmol/L pyoverdine PBS solution, with final Fe^{3+} contents being 5 μmol/L.

TABLE III Characterization data of different concentrations pyoverdine samples containing 5 μmol/L iron.

$C_{pyoverdine}$/(μmol/L)	$t_{obs.}$/min	$\langle R_h \rangle$/nm	PDI
25	10	81	0.225
	790	0	
50	10	90	0.191
	700	0	

tents in the environments play an important role in the *Pseudomonas aeruginosa* growth and pyoverdine production. Even in the iron-rich environment, *Pseudomonas aeruginosa* still need pyoverdine to dissolve the insoluble iron. To understand the mechanism of the pyoverdine combining with various types of iron can help us to prevent and treat the *Pseudomonas aeruginosa* infection.

V. ACKNOWLEDGMENTS

We thank professor Fan Jin of University of Science and Technology of China provided idea and designed the experiments. This work was supported by the National Program on Key Basic Research Project (No.2012CB933802) and the National Natural Science Foundation of China (No.21274141, No.21104071).

[1] C. Andreini, I. Bertini, G. Cavallaro, G. L. Holliday, and J. M. Thornton, J. Biol. Inorg. Chem. **13**, 1205 (2008).
[2] V. Braun, Biol. Chem. **378**, 779 (1997).
[3] K. A. Mies, J. I. Wirgau, and A. L. Crumbliss, BioMetals **19**, 115 (2006).
[4] M. Miethke and M. A. Marahiel, Microbiol. Mol. Biol. Rev. **71**, 413 (2007).
[5] P. Cornelis, Appl. Microbiol. Biotechnol. **86**, 1637 (2010).
[6] R. C. Hider and X. Kong, Nat. Prod. Rep. **27**, 637 (2010).
[7] I. J. Schalk, M. Hannauer, and A. Braud, Environ. Microbiol. **13**, 2844 (2011).
[8] J. R. Govan and V. Deretic, Microbiol. Rev. **60**, 539 (1996).
[9] A. G. Anne-Marie, S. Blanc, N. Rachel, A. Z. Ocaktan, and M. A. Abdallaht, Inorg. Chem. **33**, 6931 (1994).
[10] I. J. Schalk and L. Guillon, Environ. Microbiol. **15**, 1661 (2013).
[11] J. M. M. a. M. Abdallah, J. Gen. Microbiol. **107**, 319 (1978).
[12] G. Briskot, K. Taraz, and H. Budzikiewicz, Liebigs Annalen Der Chemie **1989**, 375 (1989).
[13] P. Demange, S. Wendenbaum, C. Linget, C. Mertz, M. T. Cung, A. Dell, and M. A. Abdallah, Biol. Met. **3**, 155 (1990).
[14] G. Mohn, K. Taraz, and H. Budzikiewicz, Z. Naturforsch. B **45**, 1437 (1990).
[15] S. Gipp, J. Hahn, K. Taraz, and H. Budzikiewicz, Z. Naturforsch. C **46**, 534 (1991).
[16] I. L. Lamont, P. A. Beare, U. Ochsner, A. I. Vasil, and M. L. Vasil, Proc. R. Soc. London, Ser. A **99**, 7072 (2002).
[17] A. Braud, F. Hoegy, K. Jezequel, T. Lebeau, and I. J. Schalk, Environ. Microbiol. **11**, 1079 (2009).
[18] J. Barrero, C. Camara, M. Perez-Conde, C. San Jose, and L. Fernandez, Analyst **120**, 431 (1995).
[19] K. Yin, W. Zhang, and L. Chen, Biosens. Bioelectron. **51**, 90 (2014).
[20] K. Yin, Y. Wu, S. Wang, and L. Chen, Sens. Actuators B **232**, 257 (2016).
[21] M. Eigen and R. Wilkins, Adv. Chem. Ser. **1**, 55 (1965).
[22] J. Y. Hamish, G. Upritchard, P. J. Bremer, I. L. Lamont, and A. James McQuillan, Langmuir **23**, 7189 (2007).
[23] P. J. B. Michael J. McWhirter, Iain L. Lamont, and A. J. McQuillan, Langmuir **19**, 3575 (2003).
[24] R. X. a. W. S. Kisaalita, Appl. Environ. Microbiol. **64**, 1472 (1998).
[25] B. Chu, *Laser Scattering*, 2nd Edn., New York: Academic Press, 84 (1991).
[26] W. Brown, *Light Scattering: Principles and Development*, Oxford: Oxford University Press, (1996).
[27] B. J. Berne and R. Pecora, *Dynamic Light Scattering: with Applications to Chemistry, Biology, and Physics*, New York: Courier Corporation, (1976).
[28] Z. Gan, J. T. Fung, M. Li, Y. Zhao, S. G. Wang, and C. Wu, Macromolecules **32**, 590 (1999).
[29] E. D. Weinberg, Microbiol. Rev. **42**, 45 (1978).
[30] J. Meyer and J. Hornsperger, Microbiology **107**, 329 (1978).

DOI:10.1063/1674-0068/30/cjcp1605114